Density functional theory study of hydrogen adsorption on Al_{12} cages

Alexander Goldberg[1] and Irene Yarovsky[2]
[1]*Accelrys Inc., 10188 Telesis Ct., San Diego, California 92121, USA*
[2]*RMIT University, GPO Box 2476V, Melbourne VIC 3001, Australia*
(Received 2 January 2007; revised manuscript received 14 February 2007; published 2 May 2007)

In this paper we present results of DFT calculations on bare and hydrogenated Al_{12} cluster with icosahedral symmetry, an atomic "cage" obtained by removing the central Al ion from the most stable Al_{13} cluster. We discuss similarities and differences between structural, energetic, and electronic properties of bare Al_{12} and hydrogenated $Al_{12}H_{12}$ and $Al_{12}H_{20}$ clusters, where the $Al_{12}H_{20}$ cluster is of particular interest for hydrogen storage application as it has a relatively high hydrogen storage capacity. We also compare structure and properties of bare and hydrogenated Al_{12} cages with the corresponding Al_{13} clusters. We found that in contrast to $Al_{13}H_{12}$ cluster the $Al_{12}H_{12}$ expands upon hydrogen adsorption on its surface. This expansion can be attributed to the missing central Al atom. Due to the cluster expansion there is more surface area available for hydrogen atoms resulting in a weakly bound but nevertheless rather stable, $Al_{12}H_{20}$ cluster. The analysis of deformation electron density reveals the covalent bonding character of $Al_{12}H_{12}$ cluster and more polar bonding in $Al_{12}H_{20}$ clusters. Clusters stability against fragmentation and their vibrational spectra are discussed.

DOI: 10.1103/PhysRevB.75.195403 PACS number(s): 36.40.Cg, 71.15.Nc, 82.33.Hk

I. INTRODUCTION

Recent reports on basic research challenges for hydrogen storage[1–3] state that developing effective hydrogen storage is a central challenge and a key factor in enabling the success of the hydrogen economy. The following operating requirements for effective hydrogen storage have been identified: (1) favorable enthalpies of hydrogen absorption and desorption; (2) quick uptake and release; (3) high storage capacity [6 wt. % target by 2010; 9.0 wt. % by 2015, specified by US Department of Energy (DOE)]; (4) effective heat transfer; (5) light weight and conservative in volume; (6) long cycle lifetime for hydrogen absorption/desorption; (7) high mechanical strength and durability; (8) safety.

Due to these considerations of performance, cost, safety and geometric limitations, there has recently been much interest in storing hydrogen gas in solid state materials such as nanostructured carbons[4–19] and light weight metal hydrides.[20–28] Recently, light metal clusters have attracted significant attention since it is believed that understanding of hydrogen interaction with such clusters could lead to design of novel hydrogen absorbing nanomaterials. Several studies on Al clusters have already been reported.[29–54]Stable Al clusters conforming to the "jellium" model, i.e., having a closed electronic shell,[55–57] have been produced experimentally[30,34,37–40] and such properties as ionization potential, electron affinities, photoelectron spectra, polarizabilities, and dissociation energies have been measured. Theoretically, Al cluster studies pertain to the elucidation of their potential energy surfaces, structural, and electronic properties and size effects.[29–36,40–54] Attempts have also been made to provide an insight into the possibilities of self-assembly of such clusters.[58–60] Detailed review of previous theoretical studies of Al clusters can be found in Ref. 61.

In our previous work,[31] we demonstrated that Al_{13} cluster in its most stable icosahedral configuration can adsorb a hydrogen atom without a potential barrier. Three stable positions were determined: atop, bridge, and hollow, with the atop position being energetically the most stable. When two hydrogen atoms were adsorbed, the structure with one atop and one bridge hydrogen has been shown to have the lowest energy. Based on this finding and the fact that the icosahedral structure comprises 20 triangular faces, 30 edges, and 12 vertices we attempted to accommodate 20, 30, 42 hydrogen atoms on the surface of Al_{13} cluster. However, all investigated $Al_{13}H_m$ (m=20,30,42) clusters have been found to possess imaginary frequencies in their ground state configuration and cannot therefore be considered stable.

In this paper we present results of DFT calculations on bare and hydrogenated Al_{12} cluster with icosahedral symmetry, an atomic "cage" obtained by removing the central Al ion from the Al_{13} cluster. In Sec. II we give details of computational method used in this study. In Sec. III we discuss similarities and differences between structural, energetic and electronic properties of bare Al_{12} and hydrogenated $Al_{12}H_{12}$ and $Al_{12}H_{20}$ clusters. We also compare structures and properties of bare and hydrogenated Al_{12} clusters with the corresponding Al_{13} clusters.

II. COMPUTATIONAL PROCEDURE

All calculations reported in this paper were performed using all electron density functional theory (DFT) code DMol[3] (Refs. 62–64). Double numerical polarized (DNP) basis set that includes all occupied atomic orbitals plus a second set of valence atomic orbitals plus polarized *d*-valence orbitals was employed. It was previously shown that all electron basis set and addition of *d* functions is essential for a proper description of high-valence Al atoms.[36] For exchange and correlation we applied the gradient corrected approach using the generalized gradient approximation (GGA) functional in the manner suggested by Perdew-Burke-Ernzerhof (PBE).[65,66] It was shown by Delley[67] that the PBE functional with the efficient DNP numerical basis set gives enthalpies of formation for a large set of tested compounds and molecules from the NIST database closer to

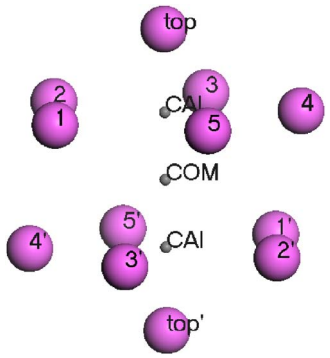

FIG. 1. (Color online) Minimum energy structure of Al_{12} cluster. Prime (′) indicates a symmetrically equivalent atom. COM - cluster center of mass; CAl - geometric center of the pentagon ring made by Al1-Al2-Al3-Al4-Al5 atoms. "Top" indicates the capping Al atom.

the experimental values than any other method available in DMol[3]. The estimated error was found to be lower than that obtained with the hybrid B3LYP/6-31G** functional.

The Gaussian smearing of electron density was applied with the energy range of 0.14 eV which enables partial occupation of electronic levels. If the electronic level is occupied with more than 0.5 e it is considered occupied in our representation.

Spin unrestricted approach was applied with all electrons being considered explicitly. In all calculations, atom centered grids were used for numerical integration with about 2000 grid points for each atom. The real space cutoff of 7.0 Å was imposed.[64]

Self-consistent-field (SCF) convergence criterion was set to the root-mean-square (rms) change in the electronic density to be less than 1×10^{-6} electron/Å^3. Geometries were optimized using an efficient algorithm taking advantage of delocalized internal coordinates.[68]

The convergence criteria applied during geometry optimization were 2.72×10^{-4} eV for energy, 0.054 eV/Å for force and 0.005 Å for displacement. For all the optimized structures we performed frequency analysis to check whether the obtained structure was a true minimum and only the true minimum structures are analyzed in this paper. In DMol[3], frequencies are evaluated by finite differences.

III. RESULTS AND DISCUSSION

A. Structural properties

The most stable Al_{12} cluster has a cage structure and possesses icosahedral symmetry. The cluster can be described as two equivalent staggered pentagon rings with a capping Al ion positioned against the center of each ring. The cluster is depicted in Fig. 1 which also shows some characteristic geometric points we use for further analysis and discussion, e.g., the cluster center of mass (COM), center of Al pentagon rings (CAl) and capping Al atoms (top). Main geometric parameters of bare and hydrogenated Al_{12} clusters are summarized in Table I. This table also contains data for Al_{13} cluster for comparison. Geometry of Al_{13} cluster was obtained with the same computational procedure described in Sec. II. Due to the symmetry all Al-Al distances (represented by Al1-Al2 ions) in Al_{12} are equivalent (2.724 Å). This is shorter than in the Al crystal where the shortest distance in the FCC lattice is 2.863 Å. It is also shorter than a corresponding distance of 2.808 Å in Al_{13} cluster. The contraction of Al-Al distance relative to Al_{13} cluster can be attributed to the lack of the repulsive central ion in Al_{12} cluster. This is further demonstrated by the fact that the distance between the central and surface Al ions in Al_{13} cluster is 2.670 Å while the distance between the center of mass (COM) and Al_s, an ion on the surface of Al_{12} cluster, is only 2.591 Å. It should also be noted that the bonding is affected by the cluster configuration as Al-Al distance in Al_2 molecule (2.653 Å) is significantly shorter than between any Al pair in the clusters considered in this paper.

TABLE I. Characteristic geometric features of bare and hydrogenated Al_{12} clusters.

Distance type[a]	Al_{12}	Al_{13}	$Al_{12}H_{12}$	$Al_{13}H_{12}$	$Al_{12}H_{20}$	$Al_{13}H_{20}$
Al1-Al2	2.724	2.808	2.729	2.785	2.737	2.968
Al-H	-	-	1.595	1.596	1.910	1.943
Al_t-CAl	1.432	1.476	1.435	1.464	1.439	1.560
Al_t-CH	-	-	0.722	0.750	0.000	0.312
CAl-CAl	2.317	2.388	2.322	2.369	2.329	2.525
CAl-CH	-	-	0.713	0.714	0.575	0.670
H-H	-	-	4.406	4.464	3.627	2.255
COM-Al_s	2.591	2.670	2.596	2.649	2.603	2.823
Al_t-H	-	-	3.817	3.871	1.910	1.943
Al_t-Al_t	5.181	5.340	5.191	5.298	5.207	5.645
H_t-H_t	-	-	8.381	8.491	6.283	6.320

[a]Used abbreviations: Al_t — Top Al atom, Al_s — Surface Al atom, H_t — Top H atom, COM — Cluster center of mass, CAl — Center of Al pentagon, CH — Center of H pentagon.

It is interesting to note that using B3LYP/LanL2DZ(d) basis set Fowler *et al.*[36] predicted Al_{12} cluster to have D_{5d} symmetry at equilibrium. We have calculated the single point energy on this geometry with our method and found it to be higher in energy than the icosahedral structure by 0.17 eV while it has no negative frequencies. The consequent geometry optimization brought it back to our lowest energy icosahedral structure. Fowler *et al.*[36] reported variations in length between three different types of Al-Al distances in their D_{5d} cluster: "peak-to-ring" (2.743 Å), "ring" (2.681 Å), and "ring-to-ring" (2.847 Å), where ring refers to Al-Al distances within the same pentagon ring and ring-to-ring refers to distances across the molecular equator. Fowler *et al.*[36] also reported another eclipsed structure classified as a saddle point rather than a true minimum. This configuration has a shorter average Al-Al distance than our minimum energy cluster with icosahedral symmetry and is a saddle point 0.90 eV higher in energy within our calculation method.

Further analysis of the bare Al_{12} cluster shows that the distance between the geometric centers of two pentagons (CAl) is 2.317 Å (2.383 Å in Al_{13}) while that between the

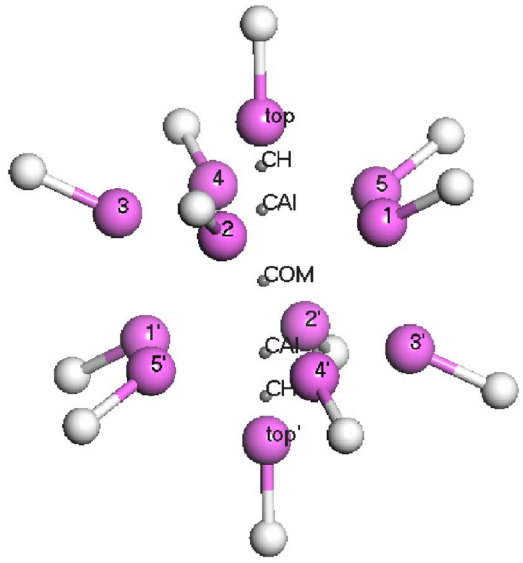

FIG. 2. (Color online) Minimum energy structure of $Al_{12}H_{12}$ cluster. Al atoms represented by large dark spheres, H atoms by small light spheres. Atom numbers are shown for Al atoms only. CH - geometric center of the pentagon ring formed by H atoms attached to Al1-5. All other abbreviations are the same as in Fig. 1.

top Al_t ion and the CAl is 1.432 Å (1.476 Å in Al_{13}), indicating the contraction of Al_{12} compared to Al_{13}. These distances will be compared to the respective distances in the hydrogenated clusters. In addition, we define the "cluster diameter" as the longest Al-Al distance; this is 5.181 Å for Al_{12} cluster and 5.340 Å for Al_{13}. Overall, it is evident from Table I that all equivalent distances between Al ions as well as between the chosen characteristic points in Al_{12} cluster are shorter than those in Al_{13} cluster.

The hydrogenated $Al_{12}H_{12}$ cluster also possesses icosahedral symmetry, with each hydrogen atom bonded to an Al ion in atop position previously reported as the most stable for the $Al_{13}H$ cluster.[31] All Al ions as well as hydrogen atoms are symmetrically equivalent in this cluster. The $Al_{12}H_{12}$ cluster is depicted in Fig. 2, also showing an additional characteristic point, CH, which is a geometric center of the ring of five hydrogen atoms attached to the Al ions forming the respective pentagons.

The measured distances between Al ions, pentagon planes and Al-H bonds in the optimized ground state $Al_{12}H_{12}$ structure are given in Table I. We note that all characteristic distances, including the shortest Al-Al distance, in the hydrogenated cluster are longer than those in the bare Al_{12} cluster, indicating that the cluster actually expands upon hydrogen adsorption. However, the Al-Al distance in $Al_{12}H_{12}$ is still shorter than the respective distance in the $Al_{13}H_{12}$ cluster. It was previously reported[43] that there is a slight reduction in the Al-Al distance with H adsorption on the lowest energy sites for some Al_nH_m ($n=6-13$, $m=1,2$) clusters. In our calculations for the $Al_{13}H_{12}$ cluster the Al-Al distance is indeed 0.023 Å shorter compared to the similar distance in the bare Al_{13} cluster. However, we do not find this in $Al_{12}H_{12}$ clusters, where the Al-Al distance is slightly longer (0.005 Å) than that in its bare Al_{12} counterpart, indicating the cluster expansion caused by adsorption.

Comparison of other characteristic distances in $Al_{12}H_{12}$ and Al_{12} clusters confirms the slight cluster expansion upon hydrogen adsorption. For instance, the distance between the top Al atom and the center of the pentagon ring is elongated from 1.432 Å to 1.435 Å in $Al_{12}H_{12}$ cluster; the distance between the centers of two pentagon rings is also increased from 2.317 Å to 2.322 Å. Note, that similar distances in $Al_{13}H_{12}$ cluster are shorter compared to its bare counterpart.

The Al-H bond length in $Al_{12}H_{12}$ cluster is 1.595 Å, significantly shorter than the bond length of 1.685 Å in the AlH molecule. This can be a result of Al atoms in clusters sharing electrons that participate in bonding with the H atom or, as was pointed out by Kawamura *et al.*,[43] due to the 3*s* electrons on Al atoms hybridizing with the 3*p* state creating a shorter bond with H. However, the Al-H distance in $Al_{12}H_{12}$ is longer than that in $Al_{13}H$ cluster with H located in the atop position (1.57 Å).[31] The Al-H bond seems to increase when more hydrogen atoms are adsorbed on the cluster surface. The effect of the central Al atom on the Al-H bond does not appear significant: the bond length is 1.596 Å in the $Al_{13}H_{12}$ cluster, which is only 0.001 Å longer than that in the $Al_{12}H_{12}$ cluster.

The distance between the top Al atom (Al_t) and the center of the hydrogen pentagon is only 0.722 Å while the distance between Al_t and each hydrogen atom in the pentagon is rather long (3.900 Å), indicating there is no bonding between these atoms. The distance between the planes of Al and H pentagons is 0.713 Å, demonstrating that H atoms are not lying within the same plane as Al. The distance between Al_t and the center of the closest hydrogen pentagon in $Al_{13}H_{12}$ cluster is longer than that in $Al_{12}H_{12}$ confirming the smaller size of the latter cluster. Although the lengths of the core Al-Al distances are different in $Al_{13}H_{12}$ and $Al_{12}H_{12}$ clusters, the Al-H bond length and the separation between the centers of Al and H pentagon rings are the same (Table I).

The longest distance between two Al ions in the $Al_{12}H_{12}$ cluster, which can be interpreted as the "inner cluster diameter," is 5.191 Å. The longest Al-Al distance in Al_{12} cluster is 5.181 Å, which indicates a slight size increase induced by the adsorbed hydrogen atoms in the $Al_{12}H_{12}$ cluster compared to the $Al_{13}H_{12}$ one. The "inner diameter" of $Al_{13}H_{12}$ cluster (5.298 Å) is smaller than the corresponding distance in the bare Al_{13} cluster (5.340 Å). This indicates that Al_{12} cluster increased in size upon hydrogen adsorption while Al_{13} cluster decreased.

The outer cluster diameter (the longest H-H distance) in $Al_{12}H_{12}$ is 8.381 Å while in $Al_{13}H_{12}$ it is 8.491 Å. Overall, all symmetrically equivalent distances in $Al_{13}H_{12}$ cluster are longer than those in $Al_{12}H_{12}$ (Table I).

The $Al_{12}H_{20}$ cluster also possesses icosahedral symmetry (Fig. 3) and provides more than 6% hydrogen adsorption capacity by weight. All hydrogen atoms are located in the hollow positions above the center of the triangle plane of Al ions typical for the icosahedral structure (Fig. 3). Every hydrogen atom belongs to threefold site with three equivalent Al-H bonds of 1.910 Å.

Similarly to the clusters reported above, all Al ions and all hydrogen atoms are equivalent. In accord with the trend ob-

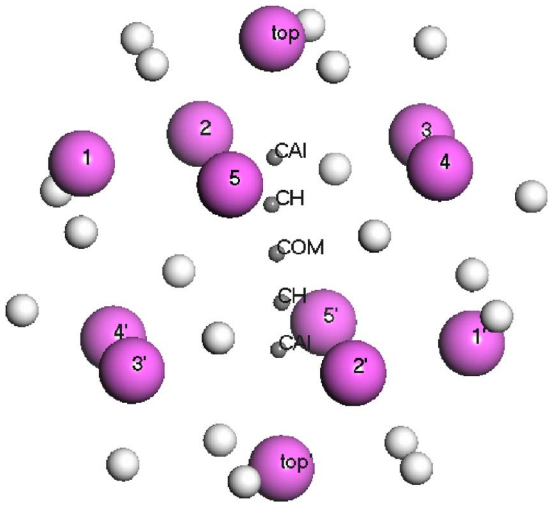

FIG. 3. (Color online) Minimum energy structure of $Al_{12}H_{20}$ cluster. All abbreviations are the same as in Figs. 1 and 2.

served for $Al_{12}H_{12}$ cluster, there is further elongation of interatomic distances in the $Al_{12}H_{20}$ cluster:

$$D(Al_{12}) < D(Al_{12}H_{12}) < D(Al_{12}H_{20}),$$

where D indicates all equivalent Al-Al distances and Al-H bond lengths. For instance, the shortest Al-Al distance in $Al_{12}H_{20}$ cluster increases to 2.737 Å. The Al-H bond length where the H position in the $Al_{12}H_{20}$ cluster is equivalent to the hollow position above the surface of Al_{13} cluster reported previously[31] is particularly long (1.910 Å). Interestingly, we found this hydrogen position to be the least stable in the $A_{13}H$ cluster with the Al-H bond length slightly longer (1.931 Å) compared to that in the $Al_{12}H_{20}$ cluster.

The top Al atom in $Al_{12}H_{20}$ is separated from the center of the Al pentagon by 1.439 Å which is slightly longer than in the $Al_{12}H_{12}$ cluster. However, in contrast to $Al_{12}H_{12}$ the hydrogen atoms and the top Al ion lie in the same plane (Fig. 3). Inner planes of Al and H pentagons are separated by 0.575 Å, being closer than in $Al_{12}H_{12}$ cluster. The H-H distance in the $Al_{12}H_{20}$ cluster (3.627 Å) is significantly shorter than that in $Al_{12}H_{12}$. The $Al_{12}H_{20}$ has the largest inner Al core with the longest Al-Al distance of 5.207 Å. However, its longest H-H separation is 6.283 Å that is 2.098 Å shorter than that in the $Al_{12}H_{12}$ cluster.

The $Al_{13}H_{20}$ cluster with icosahedral symmetry was also considered but was found to be a saddle point with a set of 16 imaginary frequencies. Comparing equivalent distances in this cluster with those in $Al_{12}H_{20}$ cluster we found that all of the Al-Al and Al-H bonds are longer in $Al_{13}H_{20}$ cluster (Table I) except that of H-H separation.

B. Energetic properties

A proper estimate of the binding energies is important in order to understand the stability against fragmentation as well as the energetics of hydrogen reaction on cluster surfaces. We calculated the total binding energy per atom using the expression

TABLE II. Calculated energetic properties of bare and hydrogenated Al_{12} clusters.

Cluster	Binding energy (eV)				HOMO-LUMO gap (eV)	IP (eV)
	Total	H	Al	AlH		
Al_{12}	2.29	-	4.08	-	1.15	5.92
Al_{13}	2.44	-	4.33 (s)[a] 4.51 (c)[b]	-	1.99	6.70
$Al_{12}H_{12}$	2.46	2.65	6.34	3.51	2.84	7.82
$Al_{13}H_{12}$	2.45	2.46	6.75 (s) 2.46 (c)	3.95	1.87	7.08
$Al_{12}H_{20}$	2.01	1.89	2.79	1.74	0.91	6.05
$Al_{13}H_{20}$	2.09	1.75	3.10 (s) 6.29 (c)	1.82	0.31	5.98

[a](s) indicates the surface Al atom.
[b](c) indicates the central Al atom.

$$E^b_{\text{total}} = \frac{E(Al_nH_m) - nE(Al) - mE(H)}{n+m},$$

where $E(Al_nH_m)$ is the total energy of the cluster, $E(Al)$ is the energy of an Al atom and $E(H)$ is the energy of an H atom. The results presented in Table II show that the cluster stability increases in the order

$$Al_{12}H_{20} < Al_{12} < Al_{12}H_{12}.$$

The binding energies of H and Al atoms as well as of the AlH molecule were calculated based on the difference in total energies of the full cluster and the cluster without the H atom or the Al atom or the AlH fragment, respectively. For instance the binding energy of the H atom was calculated as

$$E^b_H = E(Al_nH_m) - E(Al_nH_{m-1}) - E(H),$$

where $E(Al_nH_{m-1})$ is the single point energy based on the optimized intact Al_nH_m cluster.

To obtain the vertical ionization potential (IP) the energy difference between the optimized neutral cluster and its positively charged counterpart was calculated (Table II). The vertical IP for the bare Al_{12} is 5.92 eV and the HOMO-LUMO gap is 1.15 eV. The total binding energy (2.29 eV) is lower than that of the icosahedral Al_{13} cluster (2.44 eV), indicating that Al_{12} cluster is less stable. Higher stability of the Al_{13} cluster also follows from the large HOMO-LUMO gap of 1.99 eV and ionization potential of 6.70 eV. In addition, both surface and central Al ions are more stable against fragmentation in the Al_{13} cluster.

Hydrogen adsorption on the low energy sites of Al_{12} and Al_{13} surface results in the change of the cluster stabilities, with Al_{12} becoming more stable than Al_{13} upon the adsorption.

$Al_{12}H_{12}$ is the most stable of all clusters considered in this study. It has a relatively large HOMO-LUMO gap of 2.84 eV and the vertical IP of 7.82 eV which is 0.85 eV and 1.12 eV higher than those in Al_{13} clusters, respectively. In $Al_{13}H_{12}$ cluster the HOMO-LUMO gap is 0.97 eV and the IP is 0.74 eV lower than those of the $Al_{12}H_{12}$ cluster.

The total binding energy of the $Al_{12}H_{12}$ cluster (2.46 eV) is close to the value of 2.426 eV reported by Alhrihs *et al.*[29] for the Al_{13} cluster with the icosahedral symmetry. Our calculations show that it is also comparable to the binding energy of the $Al_{13}H_{12}$ cluster (Table II).

In the $Al_{12}H_{12}$ cluster each hydrogen atom is strongly bound to the Al core with the binding energy of 2.65 eV, which is slightly lower than the calculated values reported by Kawamura *et al.*[43] for the bridge and hollow hydrogen positions on the Al_{13} (2.880 and 2.867 eV, respectively). For comparison, the binding energy of H atom in the $Al_{13}H_{12}$ cluster is 0.19 eV lower than that in the $Al_{12}H_{12}$ cluster (Table II).

The binding energy of an Al atom in $Al_{12}H_{12}$ cluster is 2.26 eV higher than that in the bare Al_{12} cluster. The binding energy of the surface Al atom in $Al_{13}H_{12}$ cluster is 0.41 eV higher than in the $Al_{12}H_{12}$ cluster. However, for the central Al atom in $Al_{13}H_{12}$ cluster the binding energy is only 2.46 eV, indicating that the cage structure (a cluster with central Al atom removed) is more stable than its "parent" cluster.

The $Al_{12}H_{20}$ cluster with the I_h symmetry is the least stable among the studied clusters, with the total binding energy of 2.01 eV. Although its IP is relatively high (6.05 eV) the HOMO-LUMO gap is only 0.91 eV. The small HOMO-LUMO gap points towards the high reactivity of this cluster. This fact can be used to promote the hydrogen release from the surface of this cluster. On the other hand this cluster would be difficult to obtain experimentally as it would be highly reactive due to the small HOMO-LUMO gap. Hydrogen atom is relatively weakly bound to the threefold site on the surface of the $Al_{12}H_{20}$ cluster, with the binding energy of 1.89 eV, which is 0.76 eV lower than that in the $Al_{12}H_{12}$ cluster. It is also among the lowest compared to the typical binding energies in small Al_nH clusters reported by Kawamura *et al.*[43] In the $Al_{12}H_{20}$ cluster the binding energy of the Al atom is 3.55 eV lower than that in the $Al_{12}H_{12}$ cluster and 1.29 eV lower than that in the bare Al_{12} cluster. Although the results reported above point towards a relatively low stability of this cluster it is important to note that to the best of our knowledge this cluster represents the highest hydrogen loading of all stable studied Al clusters to date.

C. Electronic properties

It is interesting to understand the charge distribution in icosahedral Al_nH_m clusters. It was previously suggested that to exhibit magic behavior within the jellium model electron transfer must occur in Al_nH_m clusters.[43–47,55–58] For example, for Al clusters there is a discussion in the literature whether the electron transfer occurs from Al_n cluster to hydrogen or the hydrogen atom donates its electron to the Al_n framework upon adsorption onto the cluster surface. Khanna and Jena,[47] Burkart *et al.*[40] suggested the electron transfer occurs towards the Al_{13} framework in an $Al_{13}H$ cluster, in order to fill the open electronic shell of this cluster. Yong Kyu Han *et al.*[52,53] and Kawamura *et al.*[43] argued that the charge transfer from H to Al_{13} is unlikely as the IP of H is significantly higher (13.6 eV) compared to Al_{13} (6.49 eV) and there could be a charge transfer to hydrogen. The authors suggested that in contrast to the electron transfer in $Al_{13}Na$ or $Al_{13}Li$ where the alkali metal donates its electron to the hydrogenlike Al_{13} "superatom," in $Al_{13}H$ cluster the electron transfer occurs from the Al_{13} superatom to hydrogen. The $Al_{13}H$ cluster stability is attributed to a strong interaction between Al_{13}^+ and H^-, which was confirmed by the analysis of the charge density.[43] Our calculations show that IP of the Al_{12} cluster is even lower (5.92 eV). Therefore, as suggested in Refs. 43, 52, and 53 the charge transfer is most likely to occur from Al_{12} cluster to hydrogen atoms. Below we report our analysis of the charge density of the studied clusters where we found different charge distributions for the Al cluster network as well as a different degree of the charge localization on the H atoms depending on the system.

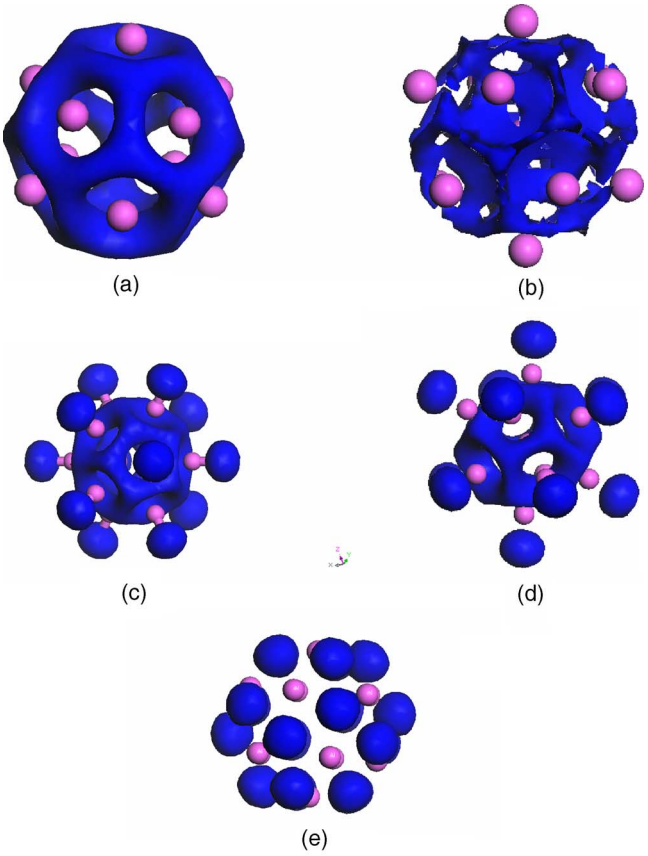

FIG. 4. (Color online) Comparison of deformation electron density of bare and hydrogenated Al_{12} and Al_{13} clusters at isovalue of 0.025 electrons/Å^3: (a) Al_{12}, (b) Al_{13}, (c) $Al_{12}H_{12}$, (d) $Al_{13}H_{12}$, and (e) $Al_{12}H_{20}$ clusters.

Electronic properties of Al_{12} cluster to a large extent are determined by its icosahedral symmetry. We analyzed the deformation of electron density of this cluster, which is calculated as the difference between the total cluster electron density and the density of the isolated atoms. The plot of the deformation electron density of Al_{12} at isovalue 0.025 electron/Å^3 [Fig. 4(a)] exhibits the delocalized character of the electronic framework of the cluster. The charge spreads over the entire cluster with high concentration between the Al ions. The deformation density of Al_{13} cluster at

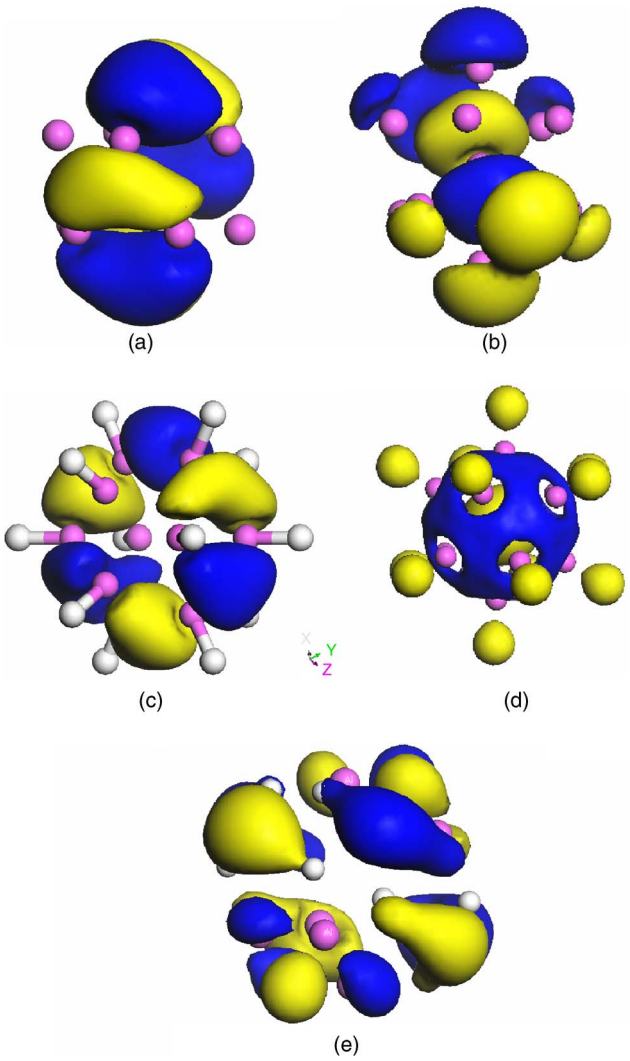

FIG. 5. (Color online) Electron density of the HOMO orbital at isovalue of 0.025 electron/Å^3: (a) Al_{12}, (b) Al_{13}, (c) $Al_{12}H_{12}$, (d) $Al_{13}H_{12}$, and (e) $Al_{12}H_{20}$ clusters.

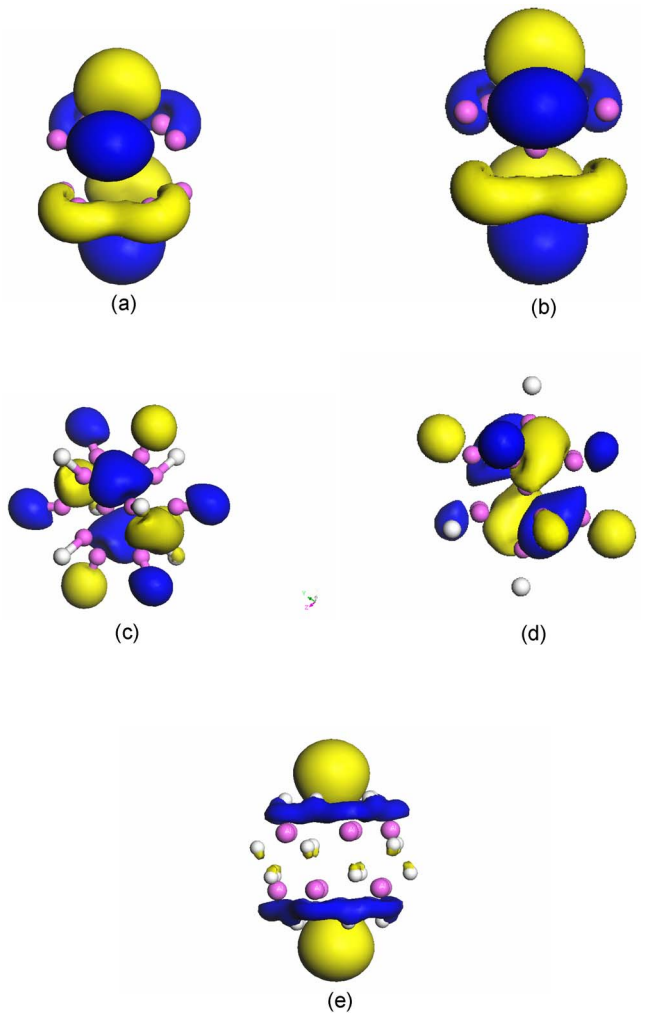

FIG. 6. (Color online) Electron density of the low energy orbitals at isovalue of 0.025 electron/Å^3: (a) Al_{12}, (b) Al_{13}, (c) $Al_{12}H_{12}$, (d) $Al_{13}H_{12}$, and (e) $Al_{12}H_{20}$ clusters.

isovalue 0.025 electron/Å^3 [Fig. 4(b)] shows slightly different character. It forms a charge network that in contrast to Al_{12} cluster is also filling the internal space of the cluster. All Al atoms in both Al_{12} and Al_{13} clusters are donating their valence electrons to shape the charge framework.

It is also interesting to investigate which orbitals contribute to the electronic cluster framework. The Al_{12} cluster has a number of degenerate orbitals resulting from the high symmetry. The one-electron HOMO orbital was identified as orbital number 154. There are 8 degenerate orbitals (147–154) that contribute to the electronic core of Al_{12} cluster. In Fig. 5(a) the Al_{12} HOMO orbital at isovalue 0.025 electron/Å^3 is presented indicating its effective delocalized character. All 8 degenerate orbitals are of similar nature and form an effective core framework of the Al_{12} cluster. Low lying electrons have more localized character. Although degenerate orbitals 141–146 contribute partially to the outer shell framework, they show more pronounced density localization around the Al ions [Fig. 6(a)]. As we show below it is these low energy electrons that are donated to hydrogen atoms to form the stable Al_nH_m clusters.

Al_{13} cluster has 6 HOMO degenerate orbitals (165–170) and consequently 8 lower lying degenerate orbitals (157–164). All these orbitals [Fig. 5(b)] signify delocalized electronic character. Lower energy orbitals (151–156) [Fig. 6(b)] exhibit localized character similarly to the Al_{12} cluster.

The deformation charge density surface at 0.025 electrons/Å^3 of the $Al_{12}H_{12}$ [Fig. 7(a)] cluster shows an excess of charge on hydrogen atoms and partially on the framework of the Al_{12} core. The 0.05 electrons/Å^3 [Fig. 7(b)] isosurface further illustrates the charge concentration on the hydrogen atoms while that on Al_{12} is considerably depleted. The picture of the higher density value (0.1 electrons/Å^3) [Fig. 7(c)] indicates significant charge around hydrogen atoms while that on Al_{12} core is completely depleted. The $Al_{13}H_{12}$ cluster follows similar trend with a few small insignificant differences.

This analysis shows the delocalization of charge from Al atoms towards the Al_{12} framework as well as the charge transfer to hydrogen atoms evident from a higher charge concentration on hydrogen atoms.

As was pointed out in the previous section the Al_{12} cluster has groups of degenerate orbitals. Eight high energy elec-

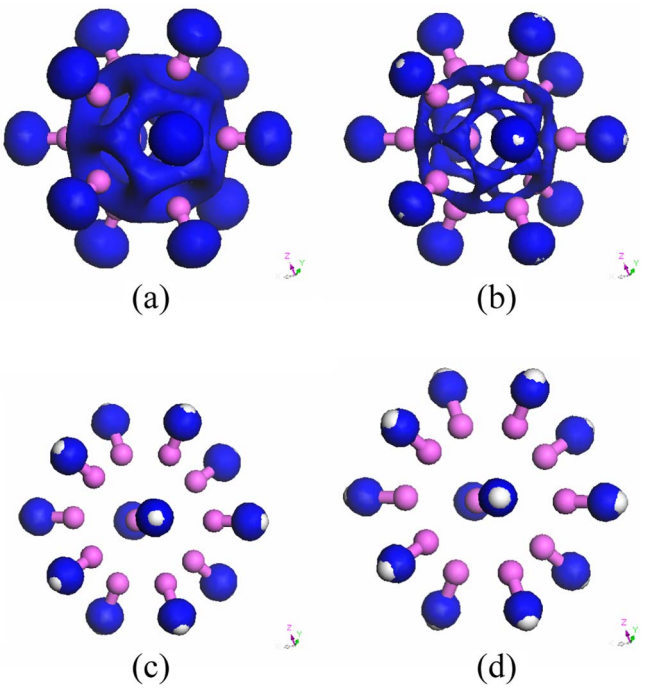

FIG. 7. (Color online) Electron deformation density surfaces of $Al_{12}H_{12}$ cluster: (a) 0.025 electrons/Å^3, (b) 0.05 electrons/Å^3, (c) 0.075 electrons/Å^3, and (d) 0.1 electrons/Å^3.

trons (orbital numbers 163–170) belong to the Al_{12} core of the $Al_{12}H_{12}$ cluster. This is evident from the similar orbital shape of the core region of the $Al_{12}H_{12}$ and bare Al_{12} clusters. Moreover there is only a small disturbance induced by hydrogen atoms to these high energy orbitals. This is illustrated by the plot of HOMO of $Al_{12}H_{12}$ cluster shown in Fig. 5(c). This orbital belongs to the $Al_{12}H_{12}$ core and is similar to the HOMO orbital of Al_{12} cluster [Fig. 5(a)].

Deep-lying degenerate electronic states of the $Al_{12}H_{12}$ cluster (numbers 153–162) are responsible for the strong covalent bonding between Al_{12} core and hydrogen atoms. These orbitals are not present in bare Al_{12} cluster. Figure 6(c) depicts the isosurface of low energy orbital (number 162) showing bonding between the Al_{12} core and the H atoms. All ten degenerate orbitals are of the same type.

The orbitals' character and the deformation electron density point to the existing polar covalent bonding between the Al_{12} core and hydrogen atoms with higher charge concentration on the hydrogen atoms.

The deformation density of the $Al_{13}H_{12}$ cluster looks similar to that of the $Al_{12}H_{12}$ cluster with some charge concentration inside the core. The nonzero charge around the cluster center can be attributed to the contribution from the central Al ion. We suggest that the expansion of the Al_{12} cluster upon adsorption of 12 hydrogen atoms is due to the missing central Al atom.

However the orbitals' shape and their order appeared to be different. There are two high energy degenerate HOMO orbitals (181–182) that are essentially shared between the central Al ion, Al_{12} core and hydrogen atoms [Fig. 5(d)]. Higher energy 8 degenerate orbitals (173–180) are similar to orbitals 163–170 in the $Al_{12}H_{12}$ cluster, i.e., these orbitals belong to

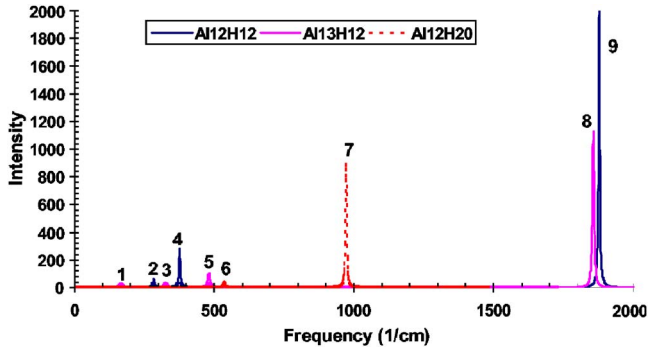

FIG. 8. (Color online) IR-Spectrum of hydrogenated Al Clusters. Peaks are labeled as follows:

Cluster/modes	Al-Al stretching	Al-H stretching	H-H vibrating
$Al_{12}H_{12}$	2	9	4
$Al_{13}H_{12}$	1,3	8	5
$Al_{12}H_{20}$	–	7	6

the Al_{12} surface. Representative orbital 180 of this type is shown in Fig. 5(d). As discussed above these orbitals appear similar to the high energy orbitals of the bare Al_{13} cluster [Fig. 5(b)].

Lower energy electrons on degenerate orbitals (163–172) contribute to covalent bonding between Al core and hydrogen atoms [Fig. 6(d)]. These orbitals are not present in the bare cluster and they are similar to degenerate orbitals (153–162) of $Al_{12}H_{12}$ cluster [Fig. 6(c)].

Overall, the orbital analysis of the $Al_{13}H_{12}$ cluster reveals polar covalent bonding between the Al core and the hydrogen atoms with the charge transfer towards the hydrogen atoms.

The $Al_{12}H_{20}$ cluster does not contain the characteristic Al_n electronic core. The 0.025 electron/Å^3 deformation density [Fig. 4(e)] shows high charge concentration around hydrogen atoms. There seems to be more charge accumulated on hydrogen atoms in comparison with the other studied clusters. In contrast to the slightly polarized covalently bonded $Al_{12}H_{12}$ cluster, the $Al_{12}H_{20}$ cluster has a pronounced ionic bonding character.

The orbitals in the $Al_{12}H_{20}$ cluster can be grouped into degenerate states, however the charge distribution of those orbitals is more delocalized. Figure 5(e) demonstrates the delocalized character of the HOMO orbital of the $Al_{12}H_{20}$ cluster. There are three degenerate HOMO orbitals (numbers 174–176). The electron density is mostly shared between each group of three atoms (H-Al-H). There are also five low energy degenerate delocalized orbitals (numbers 169–175) of a different shape [Fig. 6(e)]. One of those orbitals (number 169) exhibits some charge delocalization among hydrogen atoms in the pentagonal arrangement.

We also note that in contrast to Al_{12} and $Al_{12}H_{12}$ clusters, $Al_{12}H_{20}$ cluster possesses an uncompensated spin that is evenly distributed around the entire cluster.

D. Frequency spectrum

We now proceed to analyzing the frequency spectra of the Al_{12}, $Al_{12}H_{12}$, and $Al_{12}H_{20}$ clusters (Fig. 8). The spectra re-

veal intensity peaks at three characteristic frequencies. Peaks 1–3 can be associated with the breathing mode of Al core related to the Al-Al bond stretching; peaks 4–6 are related to the H atoms vibration around the cluster surface; peaks 7–9 are related to the Al-H bond stretching.

Since the Al-H bond is rather short the associated frequency mode has the highest energy. The stretching mode of the longer Al-Al bond has low energy. The energy of the frequency mode related to H vibration is in between those two. The obtained frequencies can be compared with those of the Al_2 and Al-H molecules. The Al-Al distance in Al_2 molecule is 2.653 Å with the characteristic frequency of about 213 cm^{-1}. Since the Al-Al distances in the studied clusters are shorter, peaks in their spectrum can be expected to arise at a higher frequency. The AlH molecule has a characteristic frequency of 1572 cm^{-1}. Al-H bonds in the considered clusters vibrate at the higher or lower frequencies depending on the Al-H bond length, i.e., $Al_{12}H_{12}$ peaks at higher energy, while the $Al_{12}H_{20}$ with the longer bond peaks at the lower energy.

Al_{12} cluster with all equivalent Al atoms has only one peak of very low intensity in its frequency spectrum (not shown in Fig. 8). This peak is associated with the symmetric stretch of Al-Al bonds and has the energy of 248 cm^{-1} which is higher than that in the Al_2 molecule, as expected. Fowler *et al.*[36] predicted a peak of the breathing mode at 257 cm^{-1} that is in a good agreement with our finding.

The $Al_{12}H_{12}$ cluster shows 3 distinct peaks: 9, 4, and 2 as labeled in Fig. 8. As expected, the highest peak corresponding to the Al-H bond breathing mode (peak 9) has a higher energy (1878 cm^{-1}) compared to the AlH molecule due to the shorter Al-H bond in the cluster. As pointed previously by Kawamura *et al.*[43] the high intensity of this peak can indicate that this hydrogen position is dynamically unstable,[43] and may, in principle, favor hydrogen desorption kinetically. The mode associated with the hydrogen atoms vibration directed around the cluster surface (labeled 4 in Fig. 8) peaks at 377 cm^{-1}. The intensity of this motion is more than seven times lower compared to the Al-H stretching mode. We can also identify a mode associated with the breathing Al-Al motion (peak 2, Fig. 8). This is a low intensity peak at 283 cm^{-1} that corresponds to the Al_{12} framework stretching mode, involving the collective motion of Al atoms. Low intensity confirms the stability of the framework against fragmentation.

The spectrum of the $Al_{13}H_{12}$ cluster has 3 peaks numbered 8, 5, and 1 in Fig. 8 with similar features to those discussed above. The mode related to the hydrogen atoms vibration directed around the cluster (peak 5) is blue shifted (energy of 482 cm^{-1}) compared to the corresponding peak of the $Al_{12}H_{12}$ cluster. Peak 8 responsible for the Al-H stretching is close in energy (1857 cm^{-1}) to the corresponding peak of $Al_{12}H_{12}$ cluster reflecting the similar Al-H bond length in the two clusters. Peaks 1 and 3 corresponding to the Al-Al stretching have energies of 165 cm^{-1} and 325 cm^{-1} respectively. The two peaks reflect the presence of two different Al-Al distances in this cluster: first, the distance between the central Al atom to the surface Al atom and, second, the distance between two closest surface Al atoms. The overall intensities of the peaks in the $Al_{13}H_{12}$ cluster are smaller indicating the higher kinetic stability of this cluster compared to the $Al_{12}H_{12}$.

In the frequency spectrum of the $Al_{12}H_{20}$ cluster the most prominent mode responsible for the stretching of Al-H bonds has a peak at 971 cm^{-1} (numbered 7 in Fig. 8). It has a lower energy than the corresponding mode in the $A_{12}H_{12}$ cluster and Al-H molecule, thus reflecting the longer Al-H bond length in the $Al_{12}H_{20}$ cluster. The intensity of this peak is less than half that in the $Al_{12}H_{12}$ cluster, pointing the dynamic stability of the Al-H bond in the $Al_{12}H_{20}$ cluster. The mode related to the H vibration with the energy of 536 cm^{-1} (labeled 6 in Fig. 8) has rather low intensity. The Al-Al stretch mode (not shown in Fig. 8) has energy of 250 cm^{-1} which is between that of the corresponding peaks in the other two clusters, reflecting the bond length order. However, due to extremely low intensity, this peak cannot be noticed in the spectrum.

IV. CONCLUSIONS

In this paper we identify stable $Al_{12}H_{12}$ and $Al_{12}H_{20}$ clusters, where the $Al_{12}H_{20}$ cluster is of particular interest for hydrogen storage as it has relatively high hydrogen storage content.

In hydrogenated clusters, characteristic Al-Al distances lengthen compared to its bare Al_{12} counterpart, indicating cluster expansion upon adsorption of hydrogen. From the comparison between Al_{12} and Al_{13} clusters we learned that in Al_{13} cluster the tendency is the opposite, i.e., the hydrogenated Al_{13} cluster contracts upon hydrogen adsorption. We can speculate that this is the reason why $Al_{12}H_{20}$ cluster is energetically stable whereas $Al_{13}H_{20}$ is not.

The expansion of the Al_{12} cluster upon adsorption of hydrogen atoms can be attributed to the missing central Al atom. The deformation electron density shows that the central Al atom in the Al_{13} cluster contributes to the electronic framework while the electronic framework of the cage cluster consists of the high electron concentration just on its surface. Consequently, in Al_{13} the electron density in the cluster interior induces reduction in the total electron density with the central atom bonding to both surface Al atoms and the hydrogen atoms. Obviously the bonding contribution from the central atom is missing in the case of the hollow cage clusters. Therefore, the cage clusters expand upon hydrogen adsorption. It should be noted that cluster expansion would play a positive role in hydrogen adsorption. Due to the cluster expansion more surface area for hydrogen adsorption becomes available resulting in a stable, although weakly bound $Al_{12}H_{20}$ cluster.

In the $Al_{12}H_{12}$ cluster all H atoms occupy the atop position while in the $Al_{12}H_{20}$ cluster they occupy the threefold site with each hydrogen atom bonded to three Al ions.

We found high energetic stability of the investigated clusters with total binding energies of 2.29 eV, 2.46 eV, and 2.01 eV, for Al_{12}, $Al_{12}H_{12}$, and $Al_{12}H_{20}$, respectively. $Al_{12}H_{12}$ cluster is the most stable, which is confirmed by an extremely high HOMO-LUMO gap and IP. The lower binding energy of $Al_{12}H_{20}$ cluster correlates with a smaller HOMO-LUMO gap. The Al_{13} cluster has a stronger binding

energy than the Al_{12}, a larger HOMO-LUMO gap and a higher IP. However, the $Al_{12}H_{12}$ cluster, having almost the same total binding energy as $Al_{13}H_{12}$, has stronger bonded H atoms, as well as a larger HOMO-LUMO gap and a higher IP.

The analysis of the deformation electron density, showed that the $Al_{12}H_{12}$ cluster is bound by polar covalent bonds between the Al_{12} core and the hydrogen atoms. The higher electron density on the H atoms indicates partial electron transfer from the Al atoms towards hydrogen upon adsorption. This feature is similar in $Al_{13}H_{12}$ cluster, although the bonding is less polarized. In contrast, the electron density of $Al_{12}H_{20}$ cluster demonstrates the ionic character of bonding in this cluster.

The electronic framework of Al_{12} cluster is found to be made of high energy electrons while low energy electrons contribute to the Al-H bonding. A similar mechanism is also found in the $Al_{13}H_{12}$, $Al_{12}H_{12}$, and $Al_{12}H_{20}$ clusters with higher electron density concentration on the hydrogen atoms in the indicated order.

The frequency spectrum analysis of the three clusters identifies the highest energy mode corresponding to Al-H stretching, followed by the H atoms vibration directed around the cluster surface and, finally, the stretching vibration mode of the Al core framework. The highest intensity corresponds to the Al-H stretching mode, indicating its dynamic instability. The lower energy mode that corresponds to hydrogen vibration has lower intensity. The low intensity of the Al core vibration points towards the high stability of the Al core for all the clusters studied.

ACKNOWLEDGMENTS

A.G. is grateful to Accelrys Inc. for supporting this research. An Australian Research Council Discovery Grant is gratefully acknowledged.

[1] Argonne National Laboratory. Report on the Basic Energy Sciences Workshop on Hydrogen Production, Storage, and Use. "Basic Research Needs for the Hydrogen Economy." May 13–15, 2003.
[2] C. Read, J. Petrovic, G. Ordaz, and S. Satyapal, Mater. Res. Soc. Symp. Proc. 885A, Warrendale, PA (2006).
[3] Report by ACIL Tasman and Parsons Brinckerhoff for Australian Government: "National Hydrogen Study," 2003.
[4] T. Yildirim and S. Ciraci, Phys. Rev. Lett. **94**, 175501 (2005).
[5] S. Dag, Y. Ozturk, S. Ciraci, and T. Yildirim, Phys. Rev. B **72**, 155404 (2005).
[6] O. Gülseren, T. Yildirim, and S. Ciraci, Phys. Rev. B **66**, 121401(R) (2002).
[7] T. Yildirim, O. Gülseren, and S. Ciraci, Phys. Rev. B **64**, 075404 (2001).
[8] O. Gülseren, T. Yildirim, and S. Ciraci, Phys. Rev. Lett. **87**, 116802 (2000).
[9] C. M. Brown, T. Yildirim, D. A. Neumann, M. H. Heben, T. Gennett, A. C. Dillon, J. L. Alleman, and J. E. Fischer, Chem. Phys. Lett. **329**, 311 (2000).
[10] A. C. Dilon, K. M. Jones, T. A. Bekkedahl, C. H. Kiang, D. S. Bethune, and M. J. Heben, Nature (London) **386**, 377 (1997).
[11] C. Liu, Y. Y. Fan, M. Liu, H. T. Cong, H. M. Cheng, and M. S. Dresselhaus, Science **286**, 1127 (1999).
[12] S. M. Lee, and Y. H. Lee, Appl. Phys. Lett. **76**, 2877 (2000).
[13] Y. Ma, Y. Xia, M. Zhao, and M. Ying, Phys. Rev. B **65**, 155430 (2002).
[14] F. Darkim and D. Levesque, J. Chem. Phys. **109**, 12 (1998).
[15] K. A. Eklund and P. C. Williams, Chem. Phys. Lett. **320**, 352 (2000).
[16] M. Siraishi, T. Takenobu, A. Yamada, M. Ata, and H. Kataura, Chem. Phys. Lett. **358**, 213 (2002).
[17] Y. Ye, C. C. Ahn, C. Witham, B. Fultz, J. Liu, A. G. Rinzler, D. Colbert, K. A. Simith, and R. E. Smalley, Appl. Phys. Lett. **74**, 16 (1999).
[18] O. Maresa, R. J.-M. Pellenq, F. Marinelli, and J. Conard, J. Chem. Phys. **121**, 12548 (2004).
[19] B. Kiran, A. K. Kandalam, and P. Jena, J. Chem. Phys. **124**, 224703 (2006).
[20] J. J. Liang, Appl. Phys. A **80**, 173 (2005).
[21] J. Liang and P. W-C. Kung, J. Phys. Chem. B **109**, 17837 (2005).
[22] J. Liang, J. Alloys Compounds (to be published).
[23] J. W. Turley and H. W. Rinn, Inorg. Chem. **8**, 18 (1969).
[24] C. Wolverton and V. Ozolins, Phys. Rev. B **73**, 144104 (2006).
[25] B. Magyari-Köpe, V. Ozolins, and C. Wolverton, Phys. Rev. B **73**, 220101(R) (2006).
[26] C. Wolverton, V. Ozolins, and M. Asta, Phys. Rev. B **69**, 144109 (2004).
[27] G. Lu and E. Kaxiras, Phys. Rev. Lett. **94**, 155501 (2005).
[28] X. Ke, A. Kuwabara, and I. Tanaka, Phys. Rev. B **71**, 184107 (2005).
[29] R. Alhirhs and S. D. Elliott, Phys. Chem. Chem. Phys. **1**, 13 (1999).
[30] M. F. Jarrold and J. E. Bower, J. Chem. Phys. **98**, 2399 (1993).
[31] I. Yarovsky and A. Goldberg, Mol. Simul. **31**, 475 (2005).
[32] A. Martinez, A Vela, D. R. Salahub, P. Calaminici, and N. Russo, J. Chem. Phys. **101**, 10677 (1994).
[33] R. O. Jones, J. Chem. Phys. **99**, 1194 (1993).
[34] M. F. Cai, T. P. Djugan, and V. E. Bondybey, Chem. Phys. Lett. **155**, 430 (1989).
[35] D. E. Bergeron, A. W. Castleman Jr., T. Morisato, and S. K. Khanna, Science **304**, 84 (2004).
[36] J. E. Fowler and J. M. Ugalde, Phys. Rev. A **58**, 383 (1998).
[37] A. Ecker, E. Weckert, and H. Schnockel, Nature (London) **387**, 379 (1997).
[38] R. E. Leuchtner, A. C. Harms, and A. W. Castleman, J. Chem. Phys. **91**, 2753 (1989).
[39] R. E. Leuchtner, A. C. Harms, and A. W. Castleman, J. Chem. Phys. **94**, 1093 (1991).
[40] S. Burkart, N. Blessing, B. Klipp, J. Muller, G. Gantefor, and G. Seifert, Chem. Phys. Lett. **301**, 546 (1999).
[41] K. Hoshino, K. Watanabe, Y. Konishi, T. Taguwa, A Nakajima, and K. Kaya, Chem. Phys. Lett. **231**, 499 (1994).
[42] A. Nakajima, K. Hoshino, T. Naganuma, Y. Sone, and K. Kaya, J.

Chem. Phys. **95**, 7061 (1991).
[43] H. Kawamura, V. Kumar, Q. Sun, and Y. Kawazoe, Phys. Rev. B **65**, 045406 (2001).
[44] V. Kumar, Phys. Rev. B **60**, 2916 (1999).
[45] J. Akola, M. Manninen, H. Hakkinen, U. Landman, X. Li, and L.-S. Wang, Phys. Rev. B **62**, 13216 (2000).
[46] F. Dukue and A. Mananes, Eur. Phys. J. D **9**, 223 (1999).
[47] S. N. Khanna and P. Jena, Chem. Phys. Lett. **218**, 383 (1994).
[48] O. P. Charkin, V. K. Kochnev, and N. M. Klimenko, Russ. J. Inorg. Chem. **51**, 1925 (2006).
[49] O. P. Charkin, N. M. Klimenko, D. O. Charkin, and A. M. Mebel, Russ. J. Inorg. Chem. **49**, 1895 (2004).
[50] O. P. Charkin, N. M. Klimenko, and D. O. Charkin, Russ. J. Inorg. Chem. **51**, 769 (2006).
[51] O. P. Charkin, N. M. Klimenko, D. O. Charkin, and A. M. Mebel, Russ. J. Inorg. Chem. **50**, 17 (2005).
[52] J. Jung and Y.-K Han, J. Chem. Phys. **125**, 064306 (2006).
[53] Y.-K Han and J. Jung, J. Chem. Phys. **125**, 084101 (2006).
[54] J. Jellinek and A. Goldberg, J. Chem. Phys. **113**, 2570 (2000).
[55] W. A. de Heer, W. D. Knight, M. Y. Chou, and M. L. Cohen, Solid State Phys. **40**, 93 (1987).
[56] W. Ekardt, Phys. Rev. Lett. **52**, 1925 (1984).
[57] M. Brack, Rev. Mod. Phys. **65**, 677 (1993).
[58] J. A. Alonso, M. J. Lopez, L. M. Molina, F. Duque, and A. Mananes, Nanotechnology **13**, 253 (2002).
[59] T. Makita, K. Doi, K. Nakamura, and A. Tachibana, J. Chem. Phys. **119**, 538 (2003).
[60] K. Doi, K. Iguchi, K. Nakamura, and A. Tachibana, Phys. Rev. B **67**, 115124 (2003).
[61] David Henry *et al.* (unpublished).
[62] B. Delley, J. Chem. Phys. **92**, 508 (1990).
[63] B. Delley, J. Chem. Phys. **113**, 7756 (2000).
[64] Accelrys, *Materials Studio, Release 4.0* (Accelrys Software, Inc., San Diego, 2006).
[65] J. P. Perdew, K. Burke, and M. Ernzerhof, Phys. Rev. Lett. **77**, 3865 (1996).
[66] J. P. Perdew, K. Burke, and M. Ernzerhof, Phys. Rev. Lett. **78**, 1396(E) (1997).
[67] B. Delley, J. Phys. Chem. A **110**, 13632 (2006).
[68] J. Andzelm, D. King-Smith, and G. Fitzgerald, Chem. Phys. Lett. **335**, 321 (2001).